INRIA

INSTITUT NATIONAL DE RECHERCHE EN INFORMATIQUE ET EN AUTOMATIQUE

Analysis of Jansen's model of a single cortical column

François Grimbert, Olivier Faugeras

N° 5597

Juin 2005

Thème BIO

ISSN 0249-6399 ISRN INRIA/RR--5597--FR+ENG

INRIA
SOPHIA ANTIPOLIS

Analysis of Jansen's model of a single cortical column

François Grimbert*, Olivier Faugeras

Thème BIO — Systèmes biologiques
Projet Odyssée

Rapport de recherche n° 5597 — Juin 2005 — 34 pages

Abstract: In this report we present a mathematical analysis of a simple model of a cortical column. We first recall some known biological facts about cortical columns. We then present a mathematical model of such a column, developed by a number of people including Lopes Da Silva, Jansen, Rit. Finally we analyze some aspects of its behaviour in the framework of the theory of dynamical systems using bifurcation theory and the software package XPP-Aut developed by B. Ermentrout. This mathematical approach leads us to a compact representation of the model that allows to finally discuss its adequacy with biology.

Key-words: cortical columns, EEG, modeling, dynamical systems, bifurcations, XPP-Aut

* **This work was partially supported by Elekta Instrument AB.**

Unité de recherche INRIA Sophia Antipolis
2004, route des Lucioles, BP 93, 06902 Sophia Antipolis Cedex (France)
Téléphone : +33 4 92 38 77 77 — Télécopie : +33 4 92 38 77 65

Analyse du modèle de colonne corticale de Jansen

Résumé : Nous présentons dans ce rapport l'analyse d'un modèle simple de colonne corticale. Nous commençons par rappeler quelques faits connus sur ces colonnes. Nous présentons ensuite un modèle mathématique de colonne, développé par un certain nombre d'auteurs dont Lopes Da Silva, Jansen, Rit. Nous analysons ensuite quelques aspects de son comportement en utilisant la théorie des bifurcations et le logiciel XPP-Aut développé par B. Ermentrout. Cette étude mathématique nous a donné une vision suffisamment compacte du modèle pour pouvoir en critiquer l'adéquation avec la biologie dans la discussion finale.

Mots-clés : colonne corticale, EEG, modélisation, système dynamique, bifurcation, XPP-Aut

Contents

1 Cortical columns

It has been hypothesized that small vertical structures called *cortical columns* are the basic units of sensory and motor information processing in the cortex. How can such a structure emerge from the complexity of the cortex?

1.1 Cortex composition and organization

The cortex is the superficial part of the encephalon and represents the biggest part of grey matter in the brain. It has a horizontal organization in layers of different types of cells (figure 1). The number of layers, their cell composition, their thickness and organization are not the same over the surface of the cortex. Those differences led neurophysiologists to divide the cortex into small regions a few square centimeters large (figure 2) where those characteristics were homogeneous and that corresponded to different functions, e.g., vision or motion. Nevertheless most of the cortex is made up of six layers of neurons, from layer I at the surface of the cortex to layer VI that lies next to the white matter. Its thickness varies from 3 to 6 mm.

About fourty types of neurons have been identified through the cortex but they can essentially be divided into only two classes: *projection neurons* and *local inter-neurons*. Projection neurons (also called *principal neurons*) are excitatory cells, most of them having a pyramidal cell body and being situated in layers III, V and VI of the cortex. Inter-neurons can be found in all layers but they just amount to 20 up to 25% of cortical neurons and are often inhibitory. Information processing in the cortex is multi-step and the axons of projection neurons carry information from one stage to the next, sometimes in distant groups of neurons. Inter-neurons can receive the same input as principal neurons but just convey it to local cells implied in the same stage of information processing. More detailed information about cortical structure and function can be found in [21, 1, 22].

1.2 Cortical columns

Neurons one runs across perpendicular to the cortex tend to be connected to each other and to respond to precise stimulations with similar activities throughout the layers, we say they form a *cortical column*.

Anatomical basis

Many cortical neurons throw their axons and dendrites from the cortex surface to the white matter thereby forming the anatomical basis of the columnar organization in the cortex (figure 3-B). Nervous fibers from the thalamus mostly end in layer IV where they are connected to stellate neurons. These neurons throw their axons towards the surface of the cortex, parallel to apical dendrites of neighboring pyramidal neurons, and establish connections with them (figure 3-C). The thalamocortical input is therefore conducted within a thin column of pyramidal cells so that the same information is shared throughout the depth of the cortex perpendicular to its surface [22].

Several studies have shown biological evidences for such small aggregates of about one hundred neurons, 20 up to 50 μm wide, called *minicolumns* [8, 30]. However the minicolumn hypothesis

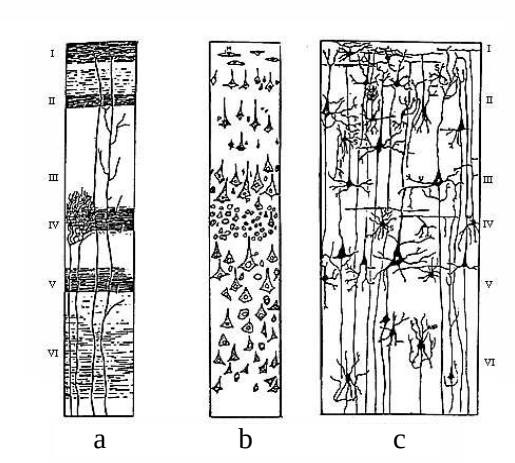

Figure 1: *Layer organization of the cortex (a) Weigert's coloration shows myelinated fibers (axons) and so the connections inside and between layers, (b) Nissl's coloration only reveals cell bodies (c) Golgi's coloration shows the whole cells (From [31]).*

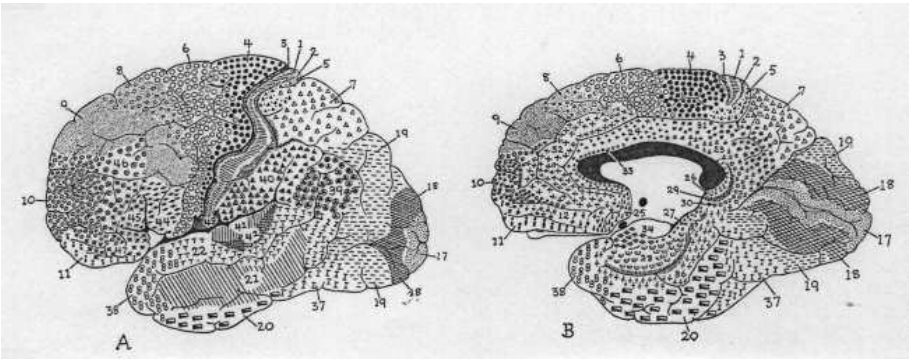

Figure 2: *In 1909, Brodmann [5] divided the cortex into 52 cytoarchitectonic areas according to the thickness of the cortical layers. For example, layer IV is very thin in the primary motor cortex (area 4) while it is very thick in the primary visual cortex (area 17).*

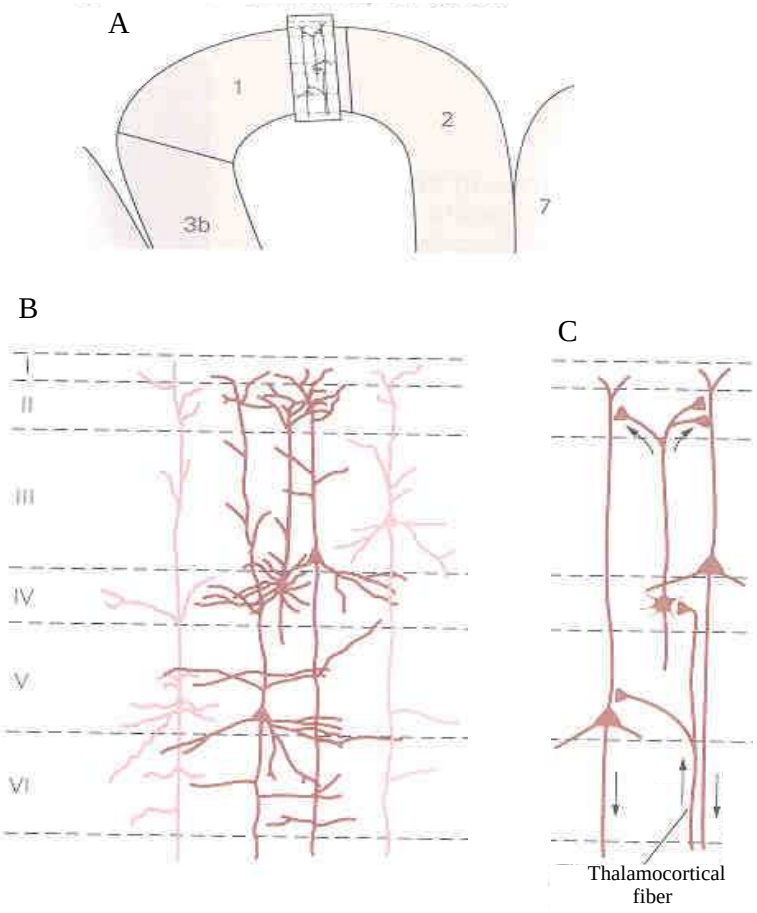

Figure 3: *(A) Sagittal section of the primary somatosensory cortex of the monkey (S-I) (B) Morphology of relay cells from layers III to V. Stellate neurons (layer IV) receive information from the thalamus and transmit it to neighboring pyramidal cells in superficial layers of the cortex. Pyramidal cells throw their axons towards deep layers of the cortex and other cortical or sub-cortical regions. They also establish horizontal connections with neighboring columns sharing the same physiological properties (C) Diagram of intra-cortical excitatory circuitry (From [22]).*

does not solve the problem of defining cortical colunms: minicolumns behaviour is not well known and horizontal connections between them tend to blur the anatomical description of larger units made up of them.

Cortical columns as physiological units

In 1957, Mountcastle discovered a columnar organization in the cortex [29] (see figure 4). With electrode recordings, he showed that neurons inside columns of 300 to 500 μm of diameter displayed similar activities. Those physiological units are usually called *macrocolumns*. In figure 5, we see physiological columns obtained from the diffusion of a radioactive substance. Some of them are spatially well defined while some ohers are more difficult to distinguish from one another. What is the meaning of such units?

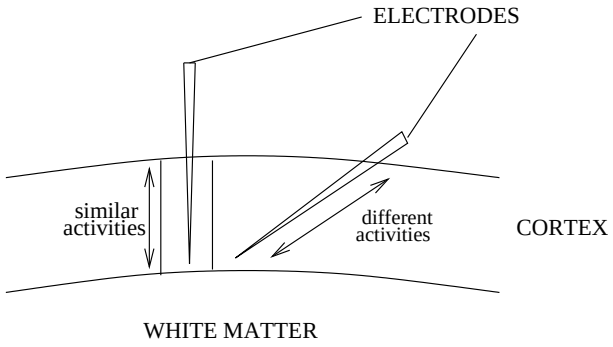

Figure 4: *Mouncastle's pioneering experiment. When he moved an electrode perpendicular to the cortex surface, he encountered neurons with similar electrical activities while moving the electrode obliquely gave him different types of recordings. So he showed the existence of 300-500 μm wide columns in the cortex.*

From physiological to functional units

Many experiments on somatosensory and visual cortices made it possible to relate physiological columns with sensory functions [22, 29, 17, 16, 28]. In some cases the processing site for a given function is clearly defined like in rat's sensory cortex where every whisker is associated with a sharply bounded cortical site in layer IV (see figure 6). In other cases, the information processing sites move continuously across the surface of the cortex when stimulation varies so that it is not possible to define a size for columns. It is the case of the *orientation columns* in the primary visual cortex (figure 7) [17, 16, 14].

So there are several non-equivalent ways to speak of a cortical column, the relevance of which strongly depends on the problem we want to tackle. For instance in the macaque monkey primary

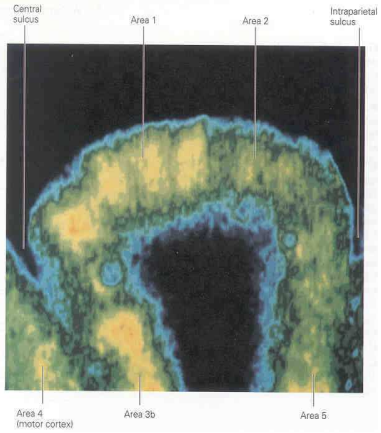

Figure 5: *Columns from the primary somatosensory cortex shown by auto-radiography after 45 minutes of stroking a hand with a brush. On this sagittal section of the cortex a high activity (proportional to the concentration of a radioactive substance) can be viewed in areas 1 and 3b. Columns are well defined in area 1 and form a continuum in area 3b (From [22]).*

visual cortex, [28] gives a very interesting discussion about both the anatomical and functional basis for columnar organization.

We now present Jansen's model of a cortical column. This model considers columns as tightly connected excitatory/inhibitory populations of neurons able to produce EEG-like activities. So if we want to link this model to biology we should consider Jansen's columns as physiological macrocolumns (0.2 to 1 millimeter wide, containing tens to hundreds of thousands cells).

2 Jansen's model of cortical columns

Jansen's model of cortical columns is based on the work of Lopes Da Silva *et al.* and Van Rotterdam *et al.* [26, 27, 35]. They developed a biologically inspired mathematical framework to simulate spontaneous electrical activities of neurons assemblies recorded by EEG, with a particular interest for alpha activity. In their model, populations of neurons interact by excitation and inhibition and can in effect produce alpha activity. Jansen *et al.* [20, 19] discovered that this model was also able to simulate evoked potentials, *i.e.* EEG activities observed after a sensory stimulation (by a flash of light, a sound, etc...). More recently, Wendling *et al.* used this model to synthesize activities very similar to those observed in epileptic patients [37].

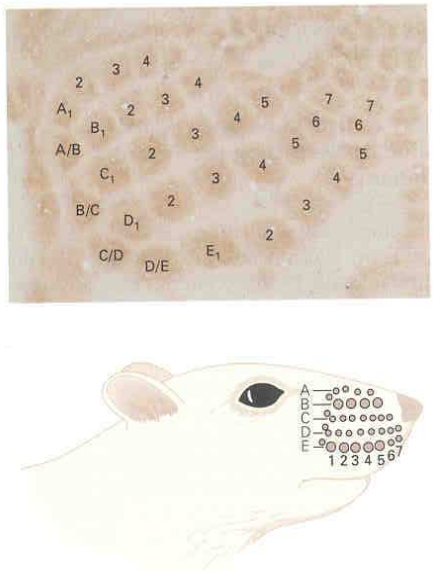

Figure 6: *Layer IV of rat's sensory cortex (stained for serotonin). Every whisker of the rat corresponds to a well defined area of the cortex mostly responsible for processing information from it. These processing units have the same distribution as whiskers on the muzzle. (From [22]).*

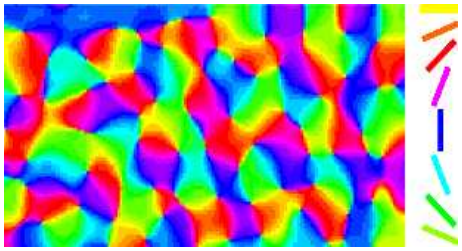

Figure 7: *A map of the visual cortex where sensitivity to the orientation of the stimulus (not to its color!) can be viewed. The legend only shows 8 directions but there is a (continuous) shading of colors on the map.*

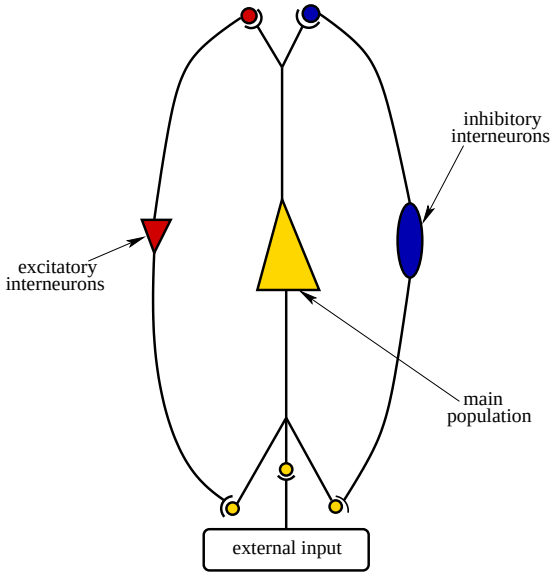

Figure 8: *Model of a cortical column: if features a population of pyramidal cells interacting with two populations of inter-neurons, one excitatory (left branch) and the other inhibitory (right branch).*

2.1 Presentation

The model features a population of pyramidal neurons (central part of figure 8) that receive excitatory and inhibitory feedback from inter-neurons residing in the same column and an excitatory input from other columns and sub-cortical structures like the thalamus. Actually the excitatory feedback must be considered as coming from pyramidal neurons themselves more than from genuine excitatory interneurons, which are not numerous in the cortex. Figure 9 is a translation of figure 8 representing the mathematical operations performed inside a column of this model. We now proceed to explain this diagram.

The excitatory input is represented by an arbitrary average firing rate $p(t)$ that can be a noise (accounting for a non specific background activity), a "peak" function simulating a flash, or signal from other columns. The three families –pyramidal neurons, excitatory and inhibitory inter-neurons– and synaptic interactions between them are modeled by different boxes.

The first kind of boxes is called *post-synaptic* ($h_e(t)$ or $h_i(t)$ in the figure: *e* stands for excitatory populations and *i* for the inhibitory ones) and converts the average rate of action potentials constituting the input of a population into an average post-synaptic potential. It converts a firing frequency into an electric potential through a second order differential linear transform whose equivalent impulse response is given by:

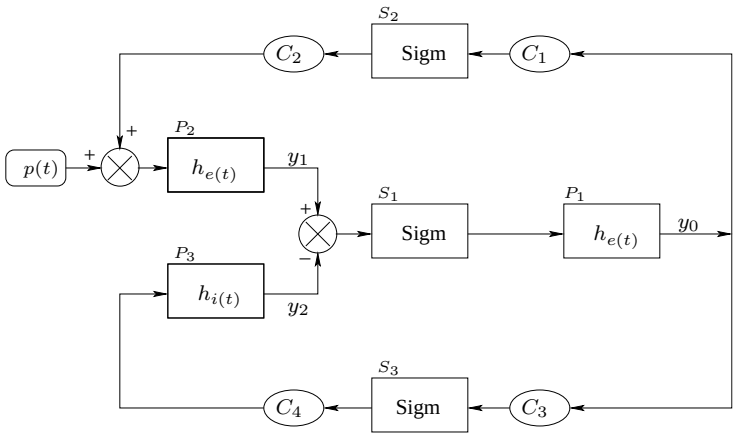

Figure 9: *Model of a cortical column. The* h *boxes simulate synapses between the neurons populations. They perform a second order differential linear transformation that converts the average firing rate of the presynaptic population into a membrane potential of the post-synaptic one. The* Sigm *boxes simulate cell bodies of neurons by transforming the membrane potential of a population into an output firing rate. This is a nonlinear transformation. The constants C_i model the strength of the synaptic connection between populations.*

$$h_e(t) = \begin{cases} Aate^{-at} & t \geq 0 \\ 0 & t < 0 \end{cases},$$

in the excitatory case and

$$h_i(t) = \begin{cases} Bbte^{-bt} & t \geq 0 \\ 0 & t < 0 \end{cases},$$

in the inhibitory one (see figure 10).

These boxes accounting for synaptic transmission have been designed by Van Rotterdam [35] in order to reproduce two characteristics of real post-synaptic potentials: shape (see figure 10) and excitatory/inhibitory ratios. Indeed, synapses made by inhibitory neurons on pyramidal cells are generally closer to the cell body than those made by the excitatory ones, resulting in an effect about ten times stronger. This has been modeled by setting proper parameters for the *h* blocks.
Each post-synaptic block corresponds to solving a differential equation such as

$$\ddot{y}(t) = Aax(t) - 2a\dot{y}(t) - a^2 y(t), \tag{1}$$

where $x(t)$ is the input of the box and $y(t)$ its output (of course one has to replace a and A by b and B for the inhibitory box). Equivalently, a system of two equations can be written

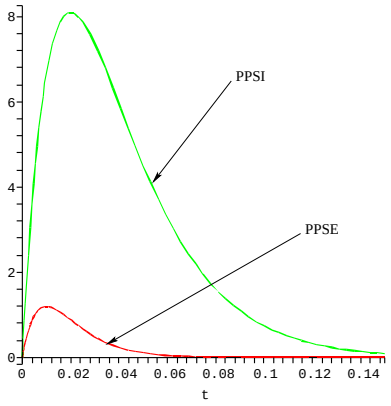

Figure 10: *The post-synaptic potentials produced by the model. The inhibitory potential (PPSI) is broader and reaches a higher maximum than the excitatory potential (PPSE), in agreement with a physiological fact: synapses established by inhibitory neurons are closer to the cell body of pyramidal cells, making their contribution about ten times stronger than that of excitatory ones.*

$$\begin{cases} \dot{y}(t) = z(t) \\ \dot{z}(t) = Aax(t) - 2az(t) - a^2 y(t) \end{cases} . \tag{2}$$

A and B determine the maximal amplitudes of the post-synaptic potentials, their units are millivolts. a and b are constants lumping together characteristic delays of the synaptic transmission, i.e. the time constant of the membrane and the different delays in the dendritic tree [12, 20]. Their units are s^{-1}.

The second type of box in Jansen's model is the *Sigmoid* that introduces a nonlinear component. This box transforms the average membrane potential of a neural population into an average firing rate. This sigmoid function has the form:

$$\text{Sigm}(v) = \frac{2e_0}{1 + e^{r(v_0 - v)}},$$

where e_0 is half of the maximum firing rate of neurons families, v_0 is the value of the potential for which a 50% firing rate is achieved (the curve has a central symmetry about the point (v_0, e_0)) and r is the slope of the sigmoid at v_0; v_0 can be viewed either as a firing threshold or as the excitability of the populations (figure 11).

This sigmoid transformation approximates the functions proposed by the neurophysiologist Walter Freeman [12] to model the conversion of the membrane potential of a family of neurons into a firing rate. This sigmoid shape models classical properties of neurons: as long as the potential is

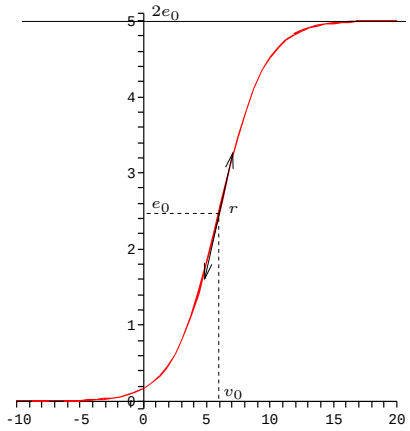

Figure 11: *Sigmoid transformation performed by the* Sigm *box that converts the membrane potential of a population into an average firing rate (abscissa in mV).*

below an excitability threshold neurons hardly produce action potentials, then, in a neighborhood of this threshold, the firing rate increases almost linearly with the surface potential until it reaches a saturation value due to the refractory period of neurons (a second action potential cannot be emitted immediately after the first one). One can therefore consider that the sigmoid box represents the average cell body action of a population by converting the membrane potential into a firing rate.

Apart from these two kinds of boxes (post-synaptic and sigmoid) the system features connectivity constants $C_1, \ldots, C_4$ that account for the number of synapses established between two neurons populations.

Let us finally discuss the variables of the system. There are three main variables noted y_0, y_1 and y_2, the outputs of the post-synaptic boxes; we also introduce their derivatives noted y_3, y_4 and y_5, respectively. If we write two equations similar to (2) for each post-synaptic block we obtain a system of 6 first order differential equations that describes Jansen's model:

$$\left\{\begin{array}{l} \dot{y_0}(t) = y_3(t) \\ \dot{y_3}(t) = Aa\text{Sigm}[y_1(t) - y_2(t)] - 2ay_3(t) - a^2 y_0(t) \\ \dot{y_1}(t) = y_4(t) \\ \dot{y_4}(t) = Aa\{p(t) + C_2\text{Sigm}[C_1 y_0(t)]\} - 2ay_4(t) - a^2 y_1(t) \\ \dot{y_2}(t) = y_5(t) \\ \dot{y_5}(t) = BbC_4\text{Sigm}[C_3 y_0(t)] - 2by_5(t) - b^2 y_2(t) \end{array}\right. . \tag{3}$$

In the next section we study the system for constant p.

2.2 Discussion: variables and constants

What do the system variables stand for?

Let us go back to figure 9. Jansen and Rit's model is intended to simulate a population of pyramidal neurons. Where are they represented in this figure? Which variables correspond to the different populations?

Let $y = y_1 - y_2$, the membrane potential of the main family of neurons. It is the input of the S_1 box which produces the average firing rate of the population that becomes the input of the P_1 box producing y_0 as an output. This output is in turn sent to the top and bottom branches of the diagram. Let us follow it in the lower, inhibitory, branch. $C_3 y_0$ is the input of the S_3 box and represents the post-synaptic potential of the inhibitory population. The output is the average firing rate of this population, which establishes an inhibitory (average) synaptic connection of strength C_4 with the main family, resulting in a contribution equal to $-y_2$ to the post-synaptic potential of the principal population at the output of P_3. A similar description can be done for the upper, excitatory, branch which also includes an excitatory input from the outside represented by the average firing rate $p(t)$.

In this model, the membrane potential of pyramidal neurons $y = y_1 - y_2$, or the resulting average firing rate (output of the S_1 box) is of special interest. We think of this quantity as the output of the column because principal neurons are the actual information transmitters from a column to another. Besides, their electrical activity corresponds to the EEG signal: pyramidal neurons throw their apical dendrites to the superficial layers of the cortex where post-synaptic potentials are summed, accounting for the essential part of EEG activity [22].

How the parameters have been set?

The parameters A, B, a and b have been determined by Van Rotterdam [35] to respect some basic properties of real post-synaptic potentials and make the system produce alpha activity. He set $A = 3.25mV$, $B = 22mV$, $a = 100s^{-1}$ and $b = 50s^{-1}$. A and B are likely to vary because certain neuropeptides modify the amplitude of post-synaptic potentials, but it is not the case for the time constants a and b, that should remain equal to these values.

The excitability of cortical neurons can vary under the action of several substances and hence v_0 could take different values, though we will use $v_0 = 6mV$ as suggested by Jansen on the basis of experimental studies due to Freeman. The works of the latter also suggest that $e_0 = 2.5s^{-1}$ and $r = 0.56mV^{-1}$, the values used by Jansen and Rit. This remains quite a crude approximation because, as shown by Freeman, the conversion of a postsynaptic potential to a firing rate made by neurons populations is not exactly a sigmoid and its characteristics vary from a population to another. [12, 13].

Let us now discuss the connectivity constants C_i, which are proportional to the average number of synapses between populations. More precisely, C_1 and C_3 account for the number of synapses established by the principal family on excitatory and inhibitory inter-neurons, respectively, while C_2 and C_4 are proportional to the number of synapses established by the excitatory and inhibitory

populations, respectively, on principal neurons. On the basis of several neuroanatomical studies ([4] among others) where these quantities had been estimated by counting synapses, Jansen and Rit managed to reduce them to a single parameter C:

$$\begin{cases} C_1 = C \\ C_2 = 0.8C \\ C_3 = 0.25C \\ C_4 = 0.25C \end{cases}$$

The parameter C is the most likely to vary under physiological constraints since it plays a part in such common synaptic phenomenons as neurotransmitter depletion.

From previous studies of Van Rotterdam and Freeman it appeared that the model could produce oscillations for $A = 3.25mV$, $B = 22mV$ and $v_0 = 6mV$. Using these values, Jansen and Rit varied C to observe alpha-like activity and obtained it for $C = 135$ (see figure 12). So their final choice of parameters to model cortical columns able to produce EEG has been

$$\begin{cases} A = 3.25 \\ B = 22 \\ v_0 = 6 \\ C = 135 \end{cases} \tag{4}$$

A word about p, which is neither a variable nor a parameter and represents the activity exterior to the column. Jansen and Rit choose $p(t)$ to be a uniformly distributed noise ranging from 120 to 320 pulses per second as they want to model non-specific input: they use the terms *background spontaneous activity*. As they simulate evoked potentials, they keep this background noise and just add a peak-like signal modeling the occurence of a flash of light. We show in the next section that studying the model for constant p already provides very important information about the behavior of the system (3). For example, this study will show that the range of the noise $p(t)$ chosen by Jansen and Rit to produce alpha activity can be explained in terms of the geometric properties of the system.

We end this discussion by commenting on the motivations that led to this choice of the parameters. Since the early works of Lopes Da Silva *et al.*, the parameters have been chosen so that the system could produce oscillations, although they tried to respect some basic biological constraints. This make us think that moving the parameters in a biologically principled manner to reproduce real behaviour will remain illusory. We will adress this issue in the Discussion at the end of the report. Now let us try to understand the mechanisms underlying the production of realistic activities by Jansen's model.

3 Bifurcations and oscillations

In this section we consider p as a parameter of the system and propose to study the behavior of a column when p varies. We therefore study the dynamical system (3) all parameters, but p, being kept constant and equal to the values set by Jansen and Rit (see (4)).

Let $Y = \begin{pmatrix} y_0 \\ \vdots \\ y_5 \end{pmatrix}$, the system has the form

$$\dot{Y} = f(Y, p),$$

where f is a smooth map from $\mathbb{R}^6$ to $\mathbb{R}^6$ and p is fixed.

We are interested in computing the fixed points and periodic orbits of the system for explaining how it can produce activities like those in figures 12 (alpha activity) and 13 (epileptic spike-shaped activities).

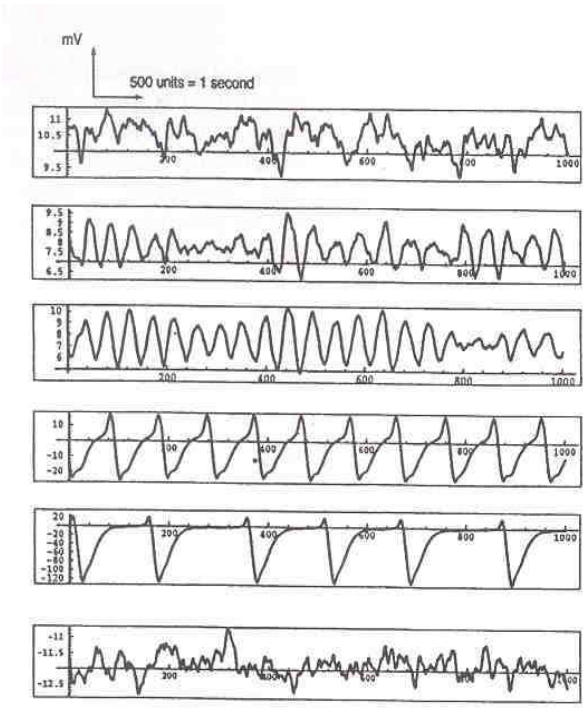

Figure 12: *Activities of a column as simulated by Jansen and Rit with a uniform noise (ranging between 120 and 320 Hz) as input. The different curves show more or less oscillatory activities depending on the value of C. The third curve from the top looks like alpha activity and has been obtained for $C = 135$ (From [19]).*

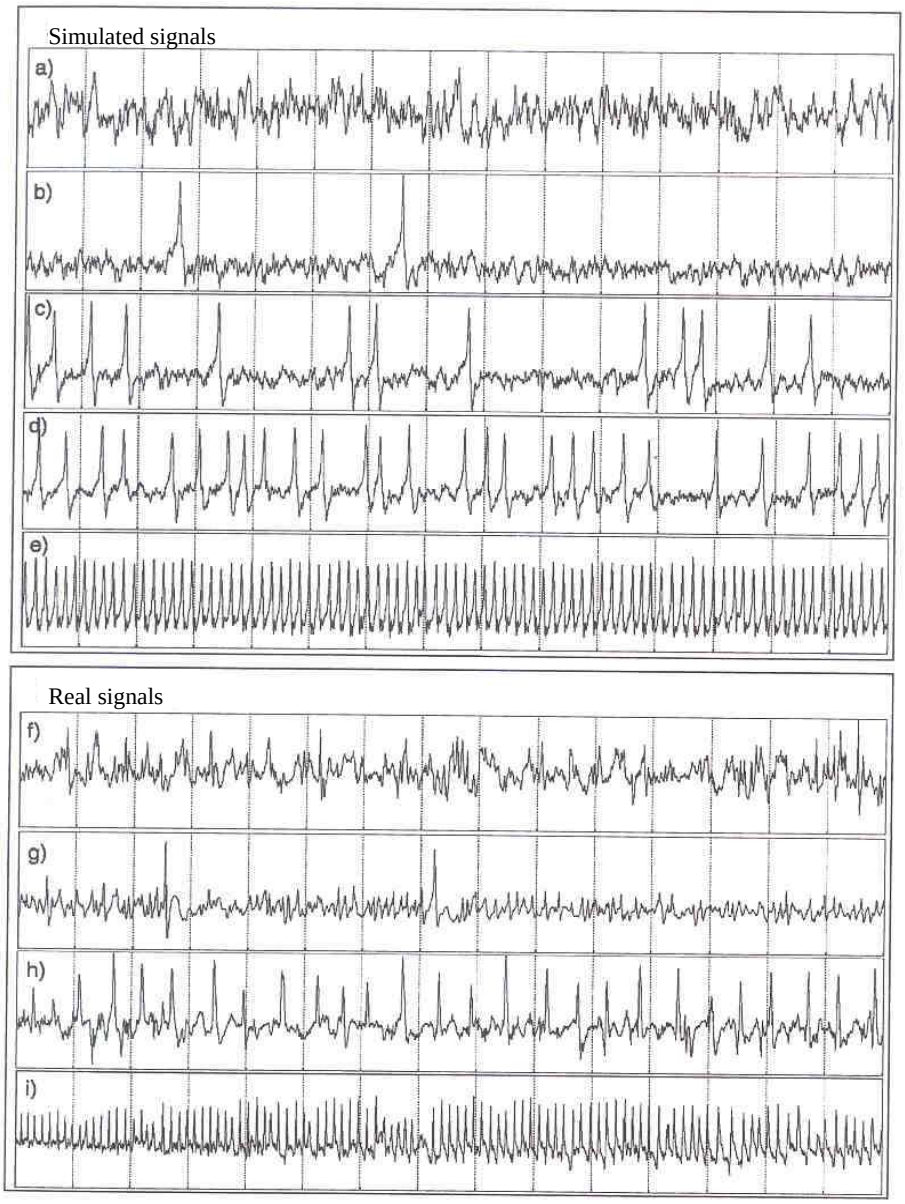

Figure 13: *(a)-(e) Activities of a column simulated with a Gaussian noise as input (corresponding to a firing rate between 30 and 150 Hz). The authors varied the excitation/inhibition ratio A/B. As this ratio is increased we observe sporadic spikes followed by increasingly periodic activities. (f)-(i) Real activities recorded from epileptic patients before (f,g) and during a seizure (h,i) (From [37]).*

3.1 Fixed points

Equation of the fixed points

We look for the points where the vector field $f(.,p)$ vanishes (called *fixed points, critical points* or *equilibrium points*). Writing $\dot{Y}=0$ we obtain the system of equations

$$\left\{\begin{array}{l} y_0 = \frac{A}{a}\text{Sigm}[y_1-y_2] \\ y_3 = 0 \\ y_1 = \frac{A}{a}(p+C_2\text{Sigm}[C_1y_0]) \\ y_4 = 0 \\ y_2 = \frac{B}{b}C_4\text{Sigm}[C_3y_0] \\ y_5 = 0 \end{array}\right. . \tag{5}$$

which leads to the (implicit) equation of the equilibrium points:

$$y = \frac{A}{a}p + \frac{A}{a}C_2\text{Sigm}\big[\frac{A}{a}C_1\text{Sigm}(y)\big] - \frac{B}{b}C_4\text{Sigm}\big[\frac{A}{a}C_3\text{Sigm}(y)\big] \tag{6}$$

As said before, $y=y_1-y_2$ represents the EEG activity of the column and p is our parameter of interest. We draw the curve of the solutions of (6) depending on y and p in figure 14.

We can already notice that for $p \approx 110-120$, the system goes from three to a single equilibrium point. Another remark: p is positive because it is a frequency. Hence parts of the graph that lie on the left side of the y axis have no meaning for our study, but play a role in the mathematical description of the model (see section 3.2).

The coordinates of the singular points cannot be written explicitely as functions of p but every singular point is completely determined by the quantity y. More precisely, the coordinates of every singular point has the following form (p and y being related through equation (6), see figure 14):

$$\left(\frac{A}{a}\text{Sigm}(y) \quad \frac{A}{a}(p+C_2\text{Sigm}[C_1\frac{A}{a}\text{Sigm}(y)]) \quad \frac{B}{b}C_4\text{Sigm}[C_3\frac{A}{a}\text{Sigm}(y)] \quad 0 \quad 0 \quad 0\right)^\top \tag{7}$$

Local study near the singular points

In order to study the behavior of the system near the fixed points we linearize the system and calculate its Jacobian matrix, *i.e.* the partial derivative $\mathcal{J}$ of $f(.,p)$ at the fixed point. It is easy to show that at the fixed point of coordinates $(y_0,y_1,y_2,0,0,0)$, we have

$$\mathcal{J}(y_0,y_1,y_2) = \begin{pmatrix} 0 & 0 & 0 & 1 & 0 & 0 \\ 0 & 0 & 0 & 0 & 1 & 0 \\ 0 & 0 & 0 & 0 & 0 & 1 \\ -a^2 & 2a\alpha(y_1,y_2) & -2a\alpha(y_1,y_2) & -2a & 0 & 0 \\ 2a\beta(y_0) & -a^2 & 0 & 0 & -2a & 0 \\ 2b\gamma(y_0) & 0 & -b^2 & 0 & 0 & -2b \end{pmatrix},$$

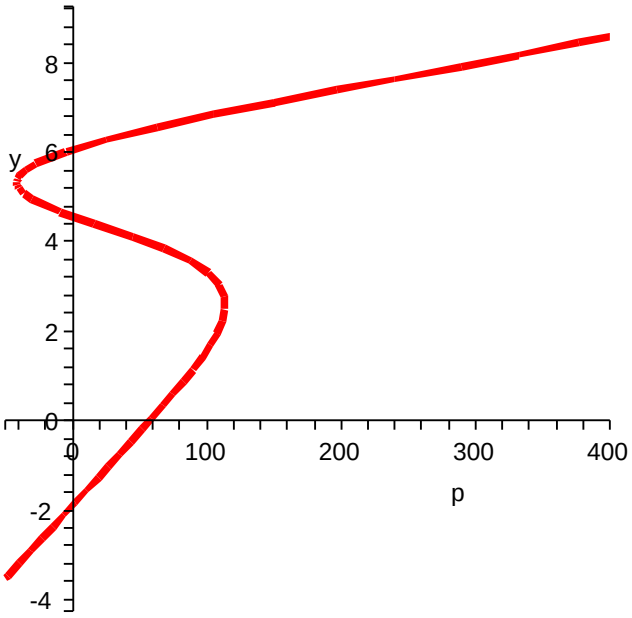

Figure 14: *Curve of the solutions of (6). For each abscissa p, we have the y('s) of the corresponding fixed point(s).*

where

$$\alpha(y_1, y_2) = \frac{A}{2}\text{Sigm}'(y_1 - y_2),$$

$$\beta(y_0) = \frac{AC_1C_2}{2}\text{Sigm}'(C_1y_0),$$

$$\gamma(y_0) = \frac{BC_3C_4}{2}\text{Sigm}'(C_3y_0).$$

Of course since the fixed point only depends on y it is also the case for its Jacobian matrix. In detail, the point $(y_0, y_1, y_2, 0, 0, 0)$ is given by (7), and hence the functions α, β and γ only depends on y. We obtain the block matrix

$$\mathcal{J}(y) = \begin{pmatrix} 0_3 & I_3 \\ KM(y) & -K \end{pmatrix},$$

where $K = \begin{pmatrix} 2a & 0 & 0 \\ 0 & 2a & 0 \\ 0 & 0 & 2b \end{pmatrix}$, $M = \begin{pmatrix} -a/2 & \alpha & -\alpha \\ \beta & -a/2 & 0 \\ \gamma & 0 & -b/2 \end{pmatrix}$, I_3 is the three-dimensional identity matrix and 0_3 the three-dimensional null matrix.

We compute the eigenvalues of the system along the curve in figure 14. The results are summarized in figure 15. The thick red portions of curve correspond to stable fixed points and thin blue to unstable fixed points. The black dots indicate that one or more eigenvalue of the system crosses the imaginary axis, having therefore a zero real part. These points are precious landmarks for the study of bifurcations of the system. Note that we have included a portion of the curve corresponding to negative values of p; indeed, despite the fact that these negative values do not have a physical meaning it turns out that the behaviour of the system for some positive values of p is determined by what happens in this part of the curve, see below.

3.2 Bifurcations and oscillatory behaviour in Jansen's model

A bifurcation is a drastic and sudden change in the behavior of a dynamic system that occurs when one or several of its parameters are varied. Often it corresponds to the appearance or disappearance of limit cycles. The description of the oscillatory behaviours in Jansen's model is therefore closely related to that of its bifurcations. When p varies from -50 to 400 and the system undergoes five bifurcations.

We now present Jansen's model bifurcations from a somewhat intuitive viewpoint but our results are solidly grounded in the mathematical theory of bifurcations [33, 18, 24, 2, 3] and could not have been obtained without the extensive use of the software *XPP-Aut* due to Bard Ermentrout (available on `http://www.pitt.edu/~phase/`).

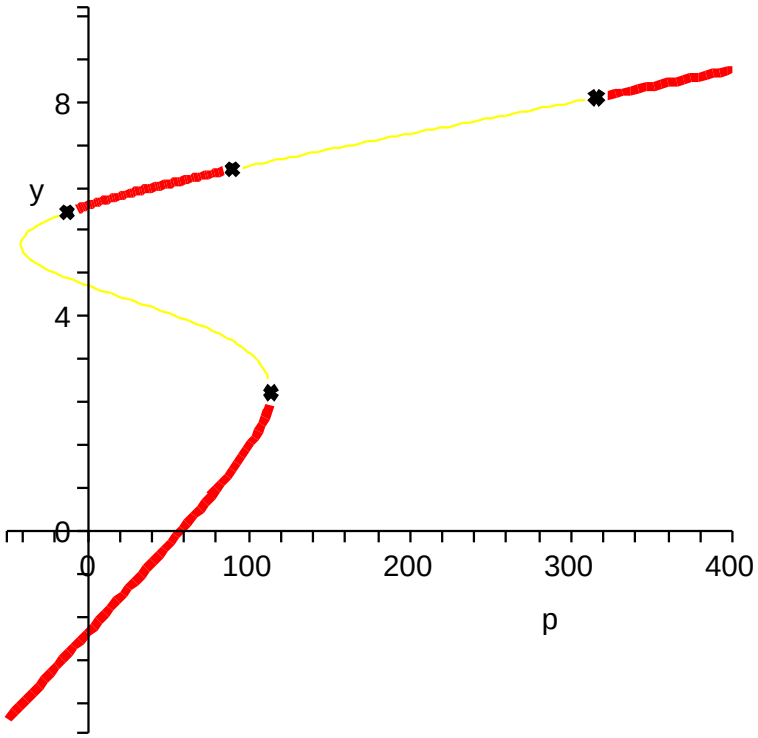

Figure 15: *Fixed points diagram of Jansen's model. The thick red portions of curve correspond to stable fixed points (all eigenvalues of the Jacobian matrix have a negative real part) while thin blue represent the unstable ones (at least one eigenvalue with positive real part). Black dots are transition points where at least one eigenvalue has a zero real part.*

Hopf bifurcations and alpha activity in Jansen's model

When p is varied smoothly the eigenvalues of the fixed points move smoothly in the complex plane: when two complex conjugate eigenvalues cross the imaginary axis one says the system undergoes a *Hopf bifurcation*. Two of them happen in Jansen's model (for $p \geq 0$), for $p = 89.83$ and $p = 315.70$. A theorem due to Hopf [33] shows [1] that for $p = 89.83$ a one parameter family of stable periodic orbits appears at the fixed point that has two complex conjugate eigenvalues crossing the imaginary axis towards positive real parts. These periodic orbits persist till $p = 315.70$ where a second Hopf bifurcation occurs: the two eigenvalues that went to the positive real part half plane return to the negative one corresponding to the (re)creation of a simple attractive fixed point. This is shown in figure 16: for p between 89.83 and 315.70, there is a family of periodic orbits (we call them *Hopf cycles* from now on) parametrized by p for which the minimal and maximal y values have been plotted (blue oval curve). The "side view" provided by figure 16 can be complemented by a "face view" in figure 17, that shows how a stable fixed point can turn into a stable periodic orbit surrounding an unstable fixed point.

Numerically, using XPP-Aut, we find that these oscillations have a frequency around 10 Hz, which corresponds to alpha activity. So it appears that alpha-like activity in Jansen's model is determined by Hopf cycles. Interestingly enough, the system does not display any Hopf bifurcation if we approximate the sigmoid by a piecewise linear function, or if we try to reduce the dimensionality of the system by singular perturbation theory [3]. In both cases the system is unable to produce alpha activity.

Let us go back to the work of Jansen and Rit. They report observing alpha activity (figure 12) when they use a uniformly distributed noise in the range 120-320 Hz at the entry of the system. This is not surprising because according to figure 16, the only attractive limit sets in this range of frequencies are (*a priori*) the Hopf cycles. So, at every time instant t the trajectories of the system will tend to coil around the Hopf cycle corresponding to $p = p(t)$, leading to the reported *waxing and waning* activity (see third curve in figure 12).

Global bifurcations and spike-like epileptic activity

Hopf bifurcations are called *local bifurcations* because their appearance only depends on local properties around the bifurcation point. In figure 13, we see that the system is able to display a spike-like activity that resembles certain epileptic EEG [37]. This spike-like activity arises from another type of bifurcation that we study now. The appearance and disappearance of the corresponding limit cycles is associated to a pair of *global bifurcations*, i.e. that do not only depend on local properties of the dynamic system.

Let us look at figure 18 where we have computed the min-max y values for this new family of cycles. The cycles begin for $p = 113.58$, where there is a *saddle-node bifurcation with homoclinic orbit*, and end for $p = 137.38$ because of a *fold bifurcation of limit cycles*.

[1] The proof of the existence of a Hopf bifurcation relies on the calculation of the *Lyapunov number* at the bifurcation points. It is quite technical and is not developed here.

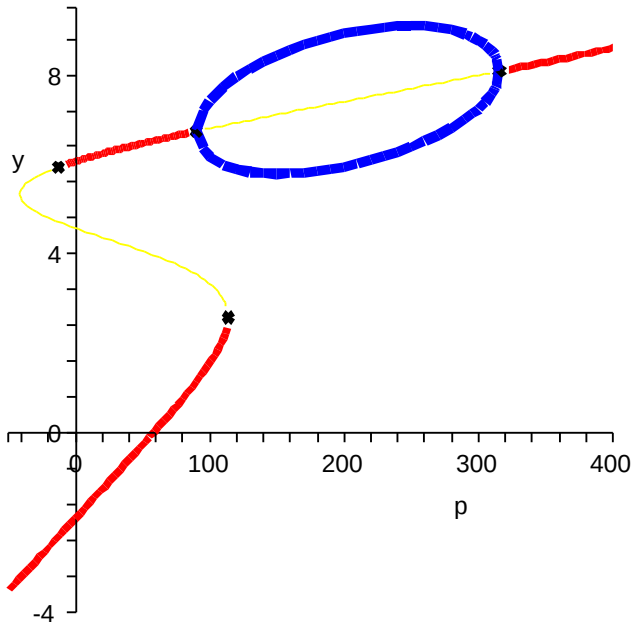

Figure 16: *Bifurcation diagram of the system for Hopf bifurcations. The thick blue oval curve represents the family of periodic orbits: it displays the lowest and highest value y attained on each limit cycle for p between 89.83 and 315.70.*

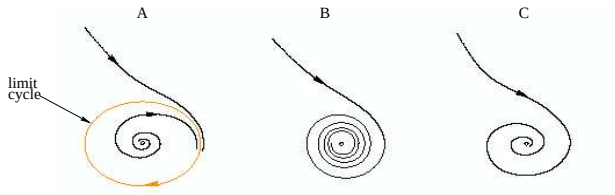

Figure 17: *This figure illustrates in two dimensions what we observe for $p = 315,70$. (A) $p < 315,70$: shrinking limit cycle (B) $p = 315,70$: the cycle has been reduced to a weak attractive point (C) $p > 315,70$: attractive fixed point. For the bifurcation occurring at $p = 89,83$ we have the same steps in reverse order (From [3]).*

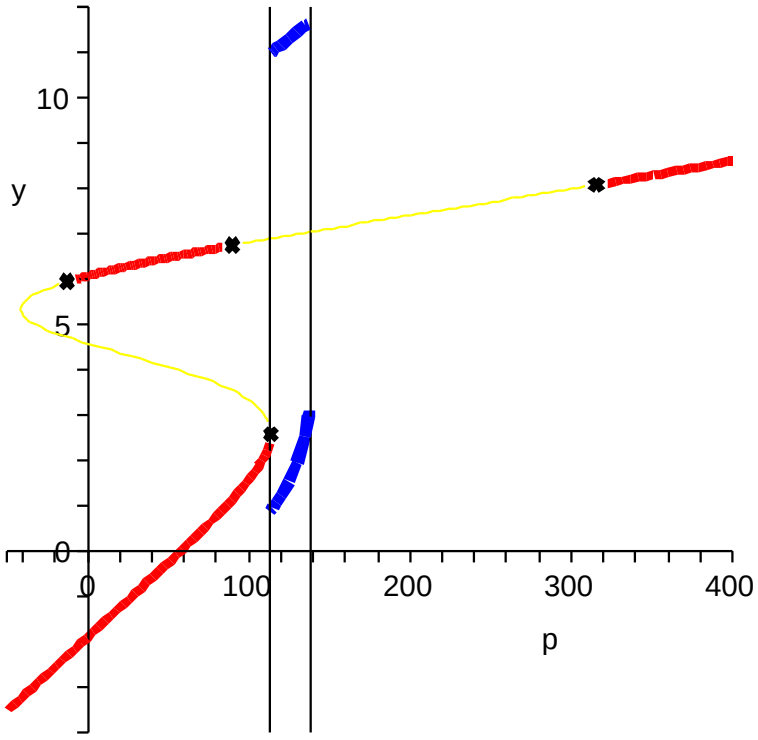

Figure 18: *Diagram of the fixed points with the min-max y values for each limit cycle of the new family. Contrary to Hopf bifurcation, the cycles appear and disappear abruptly.*

The saddle-node bifurcation with homoclinic orbit at $p = 113.58$ can be understood from figures 19 and 20 [2]. The red and green curves in figure 19 are parts of the curve in figures 14-16. The blue points represent fixed points of the dynamic system, one stable and one unstable. The thin continuous black curves with arrows represent trajectories of the system, the first one on the left is a heteroclinic orbit, turning at the saddle-node bifurcation into a homoclinic orbit (middle curve) which gives rise to limit cycles for some larger values of p (curve on the right). Figure 19 mixes 2D (fixed points) and 6D (trajectories of the system) in one diagram. The "face view" in figure 20 helps to understand this phenomenon better. There are two trajectories leaving an unstable fixed point in opposite directions and converging to a stable one (left curve in figure 19). The union of both trajectories is not a limit cycle, but as p increases one trajectory shrinks till the system has an orbit homoclinic to the point $P = (p = 113.58, y = 2.58)$, which means that any point on this trajectory will converge to P as $t \to \pm\infty$ (middle curve in figure 19). This gives rise to high amplitude genuine limit cycles for $p > 113.58$ (right curve in figure 19).

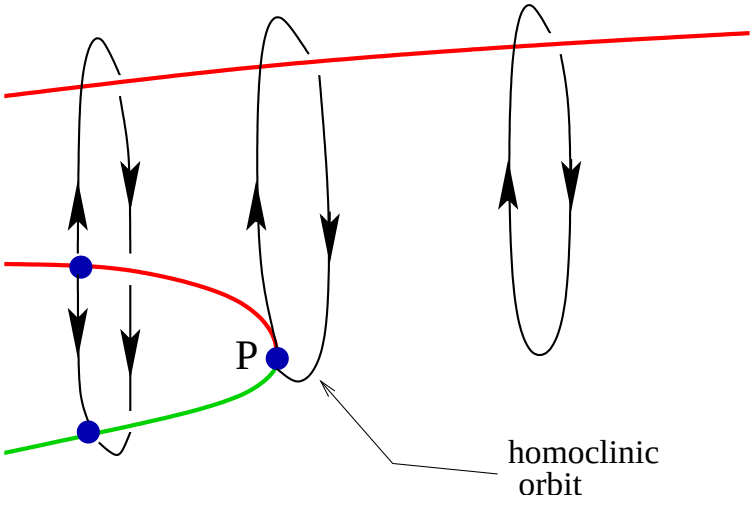

Figure 19: *Branches of fixed points in the (p, y) plane (red and green color) with 6D trajectories of the system (in black). The figure can be seen in 3D, with the trajectories lying in planes orthogonal to the curve of fixed points.*

Concerning the second global bifurcation that ends the "spiking" phenomenon (for $p = 137.38$), we identified it, thanks to XPP-Aut, as a fold bifurcation of limit cycles. It results from the fusion of a stable and an unstable family of periodic orbits (see figure 21). The unstable family originates from the Hopf bifurcation occuring at $p = -12.15$. This bifurcation corresponding to a nonphysical value of p plays nonetheless an important role in the behaviour of the dynamic system.

[2] The proof of the existence of this saddle-node bifurcation with homoclinic orbit uses a theorem due to Shil'nikov [24].

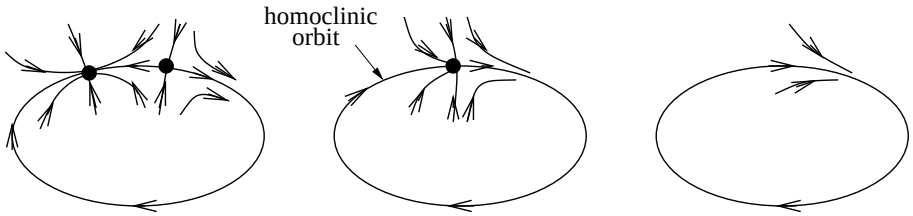

Figure 20: *"Face view" of the saddle-node homoclinic bifurcation. As p is increased, the two trajectories become a limit cycle, passing through a homoclinic orbit at the bifurcation value.*

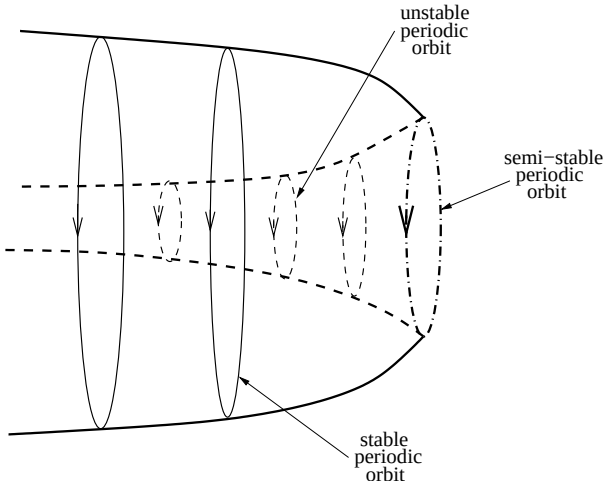

Figure 21: *Fold bifurcation due to the merging of two periodic orbits from different families. At the bifurcation value $p = 137.38$, there is a semi-stable limit cycle.*

Thanks to XPP-Aut, we have been able to compute and plot a "side view" of the folding and the associated Hopf bifurcation according to the y_0 axis (see figure 22). So far we have shown bifurcation diagrams in the (y, p) plane, but it turned out that XPP-Aut could only compute the bifurcation diagram in the (p, y_0) plane in this case. But the general properties are the same, for example we recognize the *S* shape of the fixed points diagram.

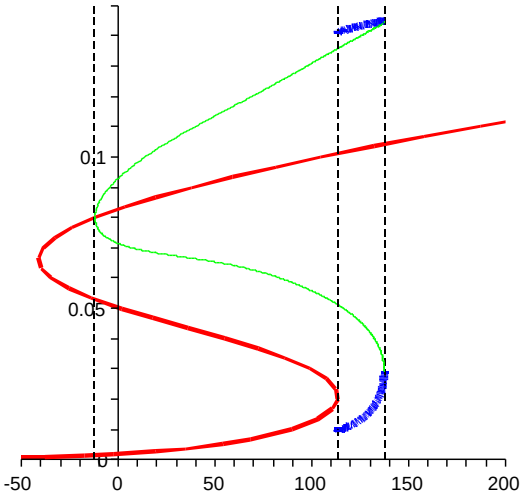

Figure 22: y_0 *plot of the three bifurcations explaining how the spike-shaped activities appear and disappear. The red S-shaped curve represents the fixed points. The green thin curve is the branch of unstable limit cycles from the Hopf bifurcation ($p = -12.15$). It merges with the branch of stable "spiking" limit cycles (blue thick curve) from the saddle-node bifurcation with homoclinic orbit, resulting in a fold bifurcation of limit cycles ($p = 137.38$).*

Contrary to the Hopf cycles whose period remains around 10 Hz, the cycles from the saddle-node bifurcation can display every frequency in the range $0 - 5$ Hz (it increases with p) so that they are able to reproduce the various "spiking" activities observed in figure 13.

Once again we can analyze the fundamental role played by p in shaping the column output. In order to produce the spikes in figure 13, Wendling *et al.* used a Gaussian noise essentially ranging from 30 to 150 Hz. For p between 30 and 90 there is a bistable behaviour with two stable fixed points, the lowest fixed point appearing to be dominant. This is due to the fact that, experimentally, the basin of attraction of the upper point is not very large, so that one has to start close to it if one wants to converge to it. As a result, a low input producesin general a low output. For p between 110 and 140, we are in the range of spike-like activity and spiking competes with Hopf cycles, but as we

will show later, trajectories starting near the low branch of fixed points (they tend to approach when $p < 100$, as said just before) will preferentially produce spikes (*i.e.* will be attracted by the global bifurcation cycles).

3.3 Synthesis: behavior of the cortical column model according to the input parameter p

We now summarize the results of our previous study by a mental experiment. Its protocole appears in figure 23. The system is stimulated by a slowly increasing linear function $p(t)$ and we look at its output $y(t)$, that represents the EEG activity.

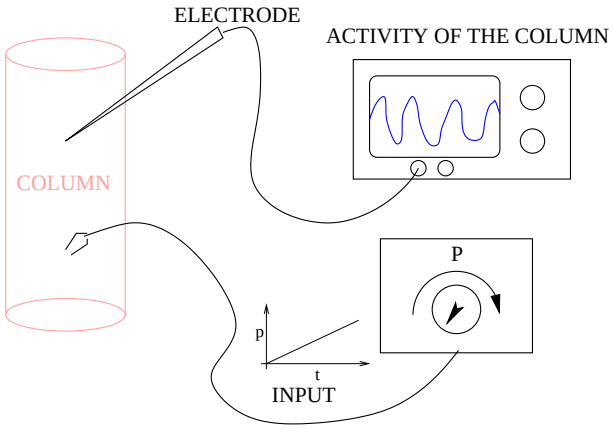

Figure 23: *Experiment. The system is stimulated with a linear function $p(t)$ (slowly increasing frequency) and we look at the time course of the EEG signal $y(t)$. In order to observe different behaviours two recordings have been made, one corresponding to the case where the initial state of the column is excited, the second corresponding to the case where the column is initially at rest.*

Figure 24 is a geometric representation of the expected behaviours for four typical values of p that is read from the bifurcation diagram. Figure 25 is a time signal representation of the same thing. For $p = 50$ the system is expected to converge toward the fixed point corresponding to the smallest value of y for an unexcited initial state and to the fixed point corresponding to the largest value of y in the case of an excited initial state. The corresponding time signals, shown in the upper lefthand part of figure 25, are "flat". For $p = 100$, if the initial state is unexcited we expect the system to converge to converge to a fixed point and if the initial state is excited, we expect the system to converge to a Hopf cycle The corresponding time signals, shown in the upper righthand part of figure 25 are a flat signal and an αrythm-like signal, respectively.. For $p = 125$, if the initial state is unexcited we expect the system to converge toward a saddle node limit cycle and if the initial state is excited we expect the system to converge to a Hopf cycle. The corresponding time signals, shown in the lower lefthand part of figure 25 are a spike-like signal and an αrythm-like signal, respectively. Finally for

$p = 200$, the system converges in both cases to a Hopf cycle, resulting in an αrythm-like signal shown in the lower righthand part of figure 25.

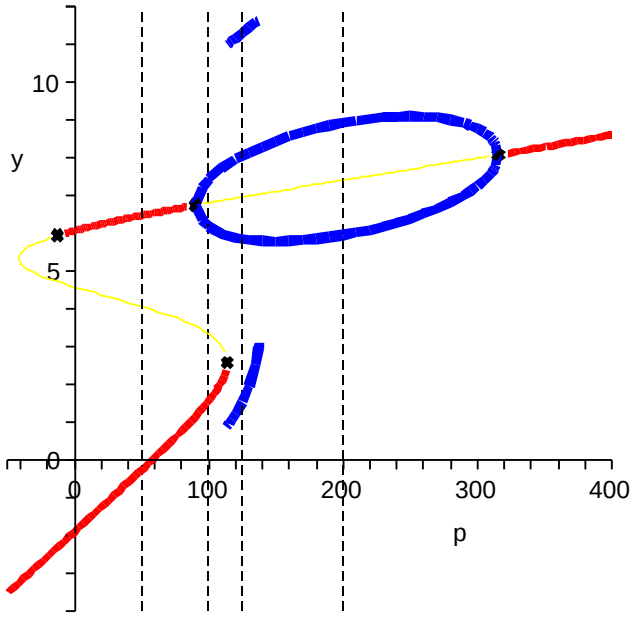

Figure 24: *Vertical black dashed lines indicate the p values for which we computed the EEG time course: $p = 50$, 100, 125 and 200 (Note: this diagram does not display the branch of unstable limit cycles occuring for $p = -12.15$). The results are shown in figure 25.*

It appears that an excited column produces alpha activity as soon as $p > 90$, while a column starting the experiment in a rest state will first "spike" (from $p \approx 110$) before it can produce alpha activity ($p > 138$).

This experiment confirms the fact that the behaviours of a column are well summarized by the bifurcation diagram (see figure 24). This geometric description gives a clear idea of the different activities the model can have and of the mathematical mechanisms underlying them.

In the light of this analysis we finally make some remarks on the adequacy of the system with biology.

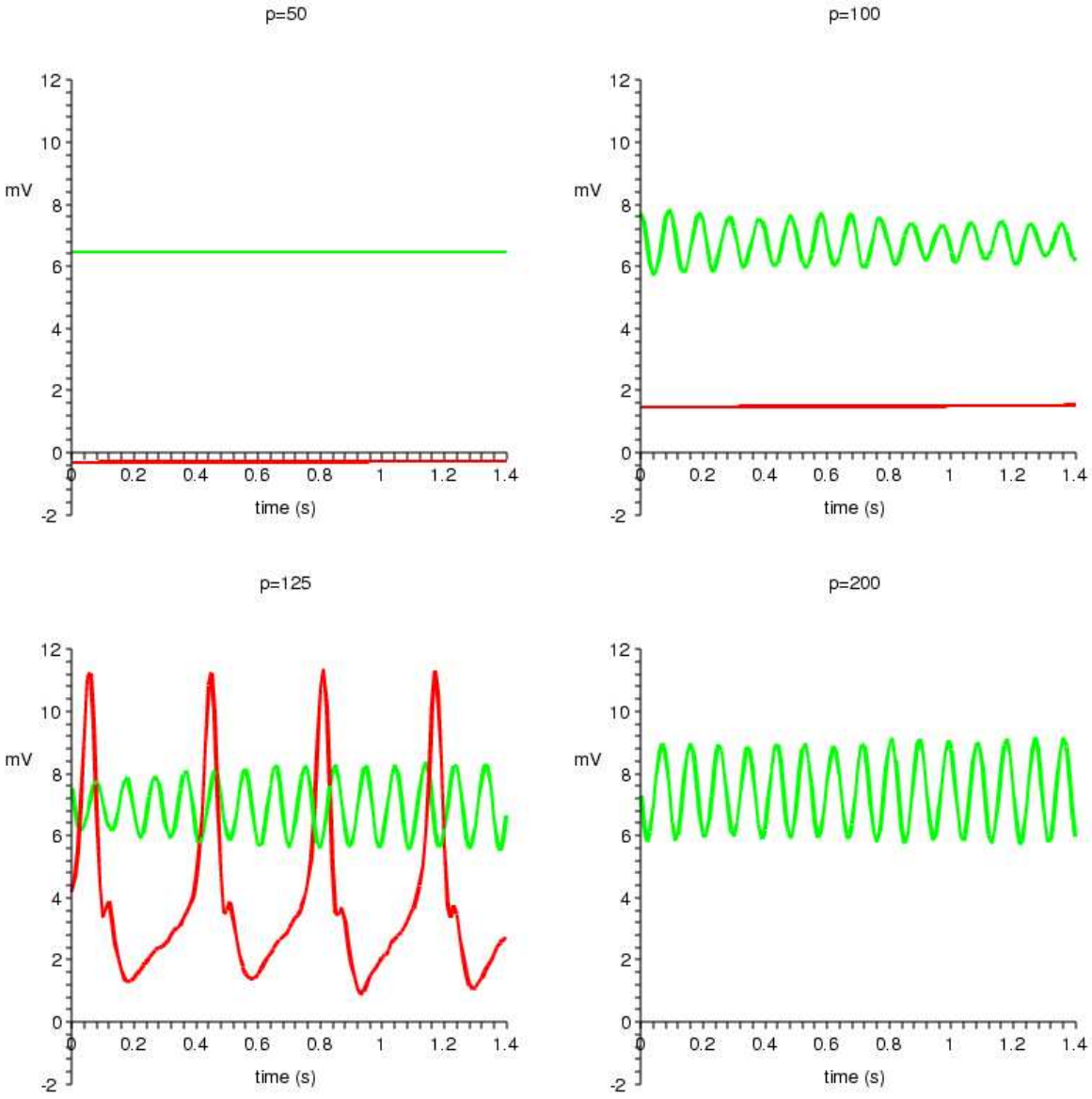

Figure 25: *Activities produced by Jansen's model for typical values of the parameter p. The green curve is the time course of an initially excited column, the red one shows the activity of an initially unexcited column. For $p > 137.38$, there is only one possible behaviour. Note: for oscillatory activities we added a very small amount of noise to the p value to make activities look more "natural" (a zero mean Gaussian noise with standard deviation 0.05).*

4 Discussion

In this section we discuss the relevance of Jansen's model. This leads to a general reflection on the difficulties of cortical column modeling.

Some remarks on the model

The model may be too simple according to one's expectations. It consists of only three neuron-like entities with a synaptic response and a cell body action, while real (macro-) columns contain tens to hundreds of thousand neurons of about fourty types with multiple ionic channels and different ways to convert their membrane potential into a firing rate.

The column can only display two types of activities (alpha and spike-like) and we do not know if they are realistic. Real assemblies of neurons produce different signals (currents, potentials, spikes synchronies, *etc*...), but the mechanisms of their production remain quite mysterious. In fact there are few results about the behaviour of a real single cortical column since it is always included in a network whose connectivities are generally not known. For example, we do not know what drives the EEG activity of a neurons assembly. Does it originate from intrinsic properties of the column, from the structure of the network the column belongs to or from the thalamic input? Probably the three origins are relevant. But it means that we do not know if a single column is supposed to produce alpha activity. Also, the intrinsic ability of the column model to produce spikes when excited in the adequate frequency band is a bit strange from a biological point of view.

Although the model has been designed from biological principles it has mainly been tuned to produce specific rhythms. Jansen's model ultimately appears as a black box capable of reproducing a few activities, mostly because of the carefully tuned properties of its bifurcation diagram rather than because of its biological relevance. When we slightly change the values of the parameters from those chosen by Jansen and Rit, the Hopf bifurcations responsible for the alpha activity disappear and the system cannot display alpha-like activity anymore. In a similar vein, David and Friston [10] were able to produce a large variety of rhythms (α, β, γ, δ and θ) with their *generalized Jansen's model* by varying the time constants and the connectivities in their equations. But as in the case of Jansen's model, their choices are largely adhoc and new approaches need to be used in order to set the parameters values in a principled manner.

Neural mass models and detailed models

Jansen's model is often said to be a *neural mass model*, a concept first introduced by Freeman [12]. It consists of several large populations of neurons modeled by a few boxes (like the *h* or *Sigm* boxes), interacting by excitation/inhibition. *Neural masses* are usually used to describe large units of the cortex or central nuclei (ranging from a few millimeters to a few centimeters wide) without worrying about either the microcircuitry between individual neurons or about a possible columnar organization. Wendling *et al.* and Lopes da Silva *et al.* used several interconnected neural masses

to simulate epileptogenic zones [25, 37, 36]. David used the same approach to study connectivities between whole cortical areas [9].
Another way to model columns consists in describing a detailed network at the scale of the neurons. Studies like that of [34, 15] are biophysically motivated and use a huge amount of data to model whole thalamocortical networks. They have been criticized [23] because they are very complex but cannot be said to be complete though. Usually detailed models restrict themselves to hundreds to a few thousands of neurons and focus on quite theoretical aspects of the network [6, 7, 11].
We think that cortical column modeling should be done at a scale between those of these two approaches. This mesoscopic scale should allow simplifications so that the model does not get trapped into irrelevant details, but carry enough precision to render specific mechanisms of columns. Our goal is to combine the two approaches and progressively produce relevant activities for good biological reasons [3].

Acknowledgements The authors thank Romain Brette and Camilo La Rota for many fruitful discussions.

References

[1] Peters A. and E.G. Jones, editors. *Cerebral cortex, cellular components of the cerebral cortex*, volume 1. Plenum, New York, 1984.

[2] N. Berglund. *Geometrical theory of dynamical systems*. Citebase, 2001.

[3] N. Berglund. *Perturbation theory of dynamical systems*. Citebase, 2001.

[4] Valentino Braitenberg and Almut Schüz. *Cortex: Statistics and Geometry of Neuronal Connectivity*. Springer, 2nd edition, 1998.

[5] K. Brodmann. *Vergleichende Lokalisationslehre der Grobhirnrinde*. J.A.Barth, Leipzig, 1909.

[6] N. Brunel. Dynamics of sparsely connected networks of excitatory and inhibitory spiking neurons. *Journal of Computational Neuroscience*, 8:183–208, 2000.

[7] N. Brunel and V. Hakim. Fast global oscillations in networks of integrate-and-fire neurons with low firing rates. *Neural Computation*, 11:1621–1671, 1999.

[8] D.P. Buxhoeveden and M.F. Casanova. The minicolumn hypothesis in neuroscience. *Brain*, 125:935–951, 2002.

[9] Olivier David, Diego Cosmelli, and Karl J. Friston. Evaluation of different measures of functional connectivity using a neural mass model. *NeuroImage*, 21:659–673, 2003.

[3] Some models do this, like the *population density approach* [32].

[10] Olivier David and Karl J. Friston. A neural mass model for meg/eeg: coupling and neuronal dynamics. *NeuroImage*, 20:1743–1755, 2003.

[11] G.B. Ermentrout and C.C. Chow. Modeling neural oscillations. *Physiology and Behaviour*, 77(4-5):629–633, 2002.

[12] W.J. Freeman. Mass action in the nervous system. *Academic Press, New York*, 1975.

[13] W.J. Freeman. Simulation of chaotic eeg patterns with a dynamic model of the olfactory system. *Biological Cybernetics*, 56:139–150, 1987.

[14] Geoffrey J. Goodhill and Miguel Á. Carreira-Perpiñán. Cortical columns. *Encyclopedia of Cognitive Science, Macmillan Publishers Ltd.*, 2002.

[15] S. Hill and G. Tononi. Modeling sleep and wakefulness in the thalamocortical system. *Journal of Neurophysiology*, 93(3):1671–1698, 2005.

[16] D.H. Hubel and T.N. Wiesel. Receptive fields, binocular interaction and functional architecture in the cat visual cortex. *J Physiol*, 160:106–154, 1962.

[17] D.H. Hubel and T.N. Wiesel. Functional architecture of macaque monkey. *Proceedings of the Royal Society, London [B]*, pages 1–59, 1977.

[18] Gérard Ioos and Moritz Adelmeyer. *Topics in Bifurcation Theory and Applications*. Advanced Series in Nonlinear Dynamics. World Scientific, 2nd edition, 1999.

[19] Ben H. Jansen and Vincent G. Rit. Electroencephalogram and visual evoked potential generation in a mathematical model of coupled cortical columns. *Biol. Cybern.*, 73:357–366, 1995.

[20] Ben H. Jansen, George Zouridakis, and Michael E. Brandt. A neurophysiologically-based mathematical model of flash visual evoked potentials. *Biological Cybernetics*, 68:275–283, 1993.

[21] E.G. Jones and A. Peters, editors. *Cerebral cortex, functional properties of cortical cells*, volume 2. Plenum, New York, 1984.

[22] E.R. Kandel, J.H. Schwartz, and T.M. Jessel. *Principles of Neural Science*. McGraw-Hill, 4th edition, 2000.

[23] N. Kopell. Does it have to be this complicated? focus on "single-column thalamocortical network model exhibiting gamma oscillations, spindles, and epileptogenic bursts". *Journal of Neurophysiology*, 93:1829–1830, 2005.

[24] Yuri A. Kuznetsov. *Elements of Applied Bifurcation Theory*. Applied Mathematical Sciences. Springer, 2nd edition, 1998.

[25] F.H. Lopes da Silva, W Blanes, S.N. Kalitzin, J. Parra, P. Suffczynski, and D.N. Velis. Dynamical diseases of brain systems: different routes to epileptic seizures. *IEEE transactions in biomedical ingeneering*, 50(5):540–548, 2003.

[26] F.H. Lopes da Silva, A. Hoeks, and L.H. Zetterberg. Model of brain rhythmic activity. *Kybernetik*, 15:27–37, 1974.

[27] F.H. Lopes da Silva, A. van Rotterdam, P. Barts, E. van Heusden, and W. Burr. Model of neuronal populations. the basic mechanism of rhythmicity. *M.A. Corner, D.F. Swaab (eds) Progress in brain research, Elsevier, Amsterdam*, 45:281–308, 1976.

[28] Jennifer S. Lund, Alessandra Angelucci, and Paul C. Bressloff. Anatomical substrates for functional columns in macaque monkey primary visual cortex. *Cerebral Cortex*, 12:15–24, 2003.

[29] V.B. Mountcastle. Modality and topographic properties of single neurons of cat's somatosensory cortex. *Journal of Neurophysiology*, 20:408–434, 1957.

[30] V.B. Mountcastle. The columnar organization of the neocortex. *Brain*, 120:701–722, 1997.

[31] John Nolte. *The Human Brain*. Mosby, 5th edition, 2001.

[32] D.Q. Nykamp and D. Tranchina. A population density approach that facilitates large-scale modeling of neural networks: extension to slow inhibitory synapses. *Neural Computation*, 13(3):511–546, 2001.

[33] L. Perko. *Differential Equations and Dynamical Systems*. Springer, 2001. Third Edition.

[34] R.D. Traub, D. Contreras, M.O. Cunningham, H. Murray, F.E. LeBeau, A. Roopun, A. Bibbig, W.B. Wilent, M.J. Higley, and M.A. Whittington. Single-column thalamocortical network model exhibiting gamma oscillations, sleep spindles, and epileptogenic bursts. *Journal of Neurophysiology*, 93(4):2194–2232, 2005.

[35] A. van Rotterdam, F.H. Lopes da Silva, J. van den Ende, M.A. Viergever, and A.J. Hermans. A model of the spatial-temporal characteristics of the alpha rhythm. *Bulletin of Mathematical Biology*, 44(2):283–305, 1982.

[36] F. Wendling, F. Bartolomei, JJ. Bellanger, and P. Chauvel. Interpretation of interdependencies in epileptic signals using a macroscopic physiological model of the eeg. *Clinical Neurophysiology*, 112(7):1201–1218, 2001.

[37] F. Wendling, J.J. Bellanger, F. Bartolomei, and P. Chauvel. Relevance of nonlinear lumped-parameter models in the analysis of depth-eeg epileptic signals. *Biological Cybernetics*, 83:367–378, 2000.

Unité de recherche INRIA Sophia Antipolis
2004, route des Lucioles - BP 93 - 06902 Sophia Antipolis Cedex (France)

Unité de recherche INRIA Futurs : Parc Club Orsay Université - ZAC des Vignes
4, rue Jacques Monod - 91893 ORSAY Cedex (France)
Unité de recherche INRIA Lorraine : LORIA, Technopôle de Nancy-Brabois - Campus scientifi que
615, rue du Jardin Botanique - BP 101 - 54602 Villers-lès-Nancy Cedex (France)
Unité de recherche INRIA Rennes : IRISA, Campus universitaire de Beaulieu - 35042 Rennes Cedex (France)
Unité de recherche INRIA Rhône-Alpes : 655, avenue de l'Europe - 38334 Montbonnot Saint-Ismier (France)
Unité de recherche INRIA Rocquencourt : Domaine de Voluceau - Rocquencourt - BP 105 - 78153 Le Chesnay Cedex (France)

Éditeur
INRIA - Domaine de Voluceau - Rocquencourt, BP 105 - 78153 Le Chesnay Cedex (France)
http://www.inria.fr
ISSN 0249-6399